Progress In Electromagnetics Research, PIER 62, 261–280, 2006

EM ENERGY ABSORPTION IN THE HUMAN BODY TISSUES DUE TO UWB ANTENNAS

M. Klemm and G. Troester

Electronics Laboratory
Department of Information Technology and Electrical Engineering
Swiss Federal Institute of Technology (ETH) Zürich
Gloriastrasse 35, 8092 Zürich, Switzerland

Abstract—This paper presents electromagnetic energy absorption in the homogeneous and layered human body models due to body-worn UWB antennas, at frequencies of 3, 6 and 8 GHz. Typical small planar UWB antennas are used in this study: printed UWB disc monopole and UWB slot antenna. Distances of 2, 5 and 10 mm (reactive near-field region) between antennas and human body were chosen, approximating realistic scenarios of operation in Wireless Body Area Networks. To approximate different parts of the human body, or body variations among different users, we compare results obtained for the planar homogeneous (muscle) model with those for three-layer body models (skin, fat and muscle), with different thicknesses of the skin (0.5–2 mm) and fat (1–9 mm) tissue. For these body models we investigate the electromagnetic energy absorption mechanism by examining the peak 1-g SAR and peak SAR (without mass averaging). Based on our results we present and discuss new finding concerning the general electromagnetic energy absorption mechanism in human tissues under reactive near-fields exposure conditions.

1. INTRODUCTION

Interaction between electromagnetic fields (EMF) and a human body has been of interest to the scientific community for a long time [1–5], and gained a tremendous attention after the introduction of cellular phones [6, 7]. In a case of mobile phones, of the main concern was the interaction between terminal antennas and a human head [8, 9].

Recently, after the introduction of wearable computing and body-centric networks (both are the part of Wireless Body Area Network - WBAN) additional factors and scenarios must be considered for compliance testing.

There is a big interest in finding a proper technology to provide a wireless connectivity for such systems. Ultra-wideband (UWB) technology is foreseen as one of the main candidates for a wireless interface in WBANs [11, 12]. Main advantages of UWB are potentially high data rates, low power consumption and restricted (by standardized bodies, e.g., FCC) levels of emitted power. Antennas play a critical role in the UWB communication systems, since they act as pulse-shaping filters [13]. In UWB WBANs or Body-Centric Networks design of the wearable UWB antenna is a major issue, thus there is a growing interest among researchers in this topic [14–18]. But also other wireless technologies (e.g., Bluetooth, WLAN, 802.11) are potentially attractive in wearable systems [19–23]. These new wireless systems will operate at higher frequencies, between 3 and 10 GHz.

Generally, most of the studies have concentrated on the evaluation of the power absorbed in the human body and a specific absorption rate (SAR). Not many studies were devoted to the understanding of the absorption mechanism in the human body. An excellent contributions in the field of electromagnetic energy absorption from '80s can be found in [3, 4], and most recent in [6, 24]. A well know absorption mechanism first published by Kuster [6] (for the homogeneous body model), were recently questioned by a controversial paper from Kivekas [25] (author has considered both homogeneous and layered body models).

In this paper we study interactions of the typical UWB antennas used in wearable applications, and different (homogeneous and layered) human body models. To approximate typical scenarios in WBANs, we assume reactive near-field exposure conditions. The main aims of this paper are to investigate the influence of body modeling of SAR results, for very small distances between an antenna and body. Our results are general and hold not only for body exposure to UWB antennas, but also for other body-worn antennas. Motivated by still arising discussions concerning a general absorption mechanism in human tissues, we investigate also this topic. New finding about the absorption in layered body tissues under reactive near-fields exposure are disclosed in this research.

2. UWB ANTENNAS

For our studies we have chosen two representative, well known planar UWB antennas: UWB slot antenna (size $32\times29\times1.5\,\mathrm{mm}^3$) and UWB

disc monopole (size $20\times37\times0.5\,\mathrm{mm}^3$). We have analyzed the same antennas in the context of UWB mobile terminals in [26]. In this study we use them only as the *tools*. These antennas are commonly used in UWB applications [27, 28]. In free-space they have quasi-omni-directional radiation pattern. Both antennas and their return loss (RL) and transmit transfer functions (H_{Tx}) characteristics are presented in Fig. 1. As we can see from the RL characteristics, both antennas has similar RL at lower frequencies (below 6 GHz), but significantly different above 6 GHz. In this study we are not really interested in comparing the performance of these two antenna. We are rather interested to see if they behave (interact) in the same manner with different models of the human body.

3. HUMAN BODY MODELING

In our studies we use two different types of the human body model. The first one is a simple homogeneous model, composed only of the muscle tissue. The second one is a three-layer model, consisting of skin, fat and muscle tissue layers. This layered model can quite well represent most of the body regions, since the fat has similar properties to the bone tissue, and the electrical parameters of the muscle and many inner organs are alike. The inclusion of the low water content fat layer, which has significantly lower dielectric constant (ϵ_r) and conductivity (σ) than the skin and muscle, is important considering the interactions of electromagnetic waves (thus also antennas) with body [3]. Due to the wave impedance mismatch between low (fat)and high (skin, muscle) water content tissues, significant reflections occur for far field exposure. This effect, can lead to the increased specific absorption rate (SAR) and does not occur in the homogeneous model.

In this paper we assume all models to be planar, and that the curvature of the body can be neglected in the case of physically small antennas. Overall surface size of all models is the same: $120\times120\mathrm{mm}^2$. The thickness of the muscle tissue is 50 mm for all models. For layered models, a thickness of the skin is 0.5, 1 and 2 mm, a thickness of the fat is 1, 3, 6 and 9 mm. These values are anatomically correct and can represent significant part of the human body [3]. All together, we have investigated 13 different body models. The electrical parameters of the tissues were assumed to be as in [29].

4. RESULTS

All results were obtained from the extensive full-wave electromagnetic simulations, using commercial solver CST Microwave Studio. Driven

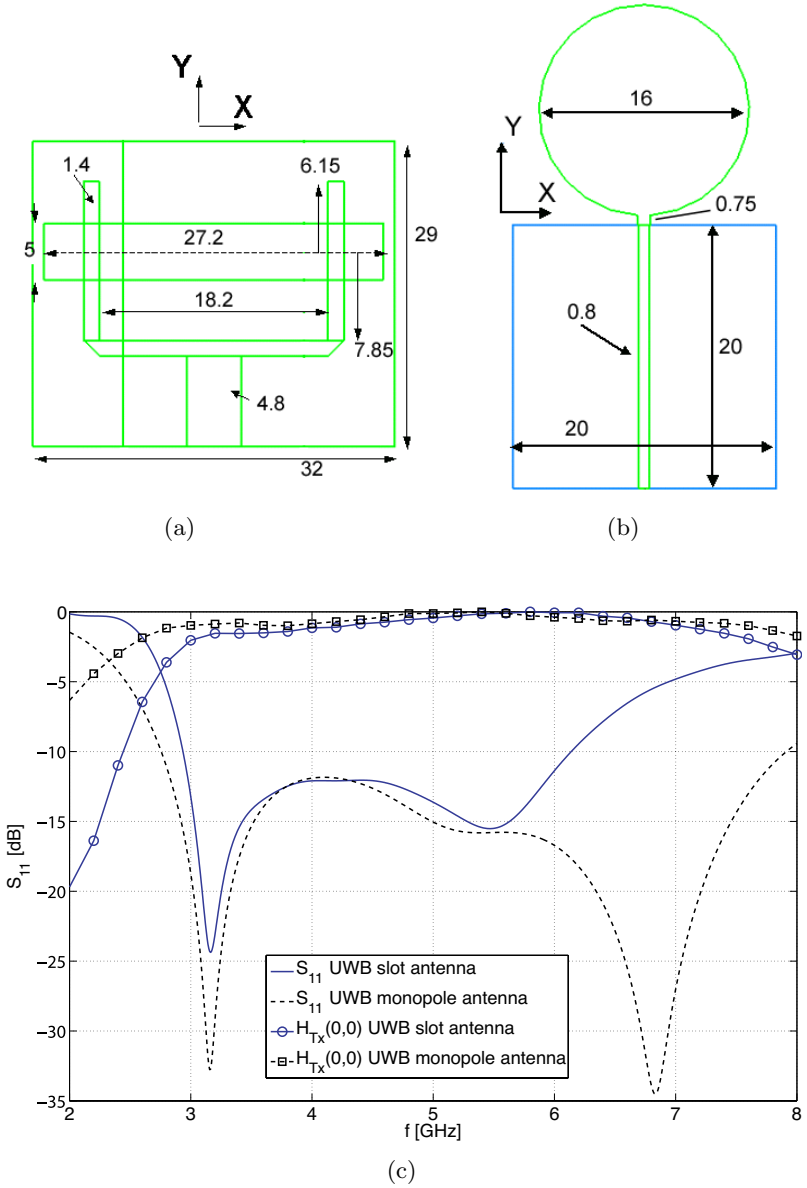

Figure 1. (a) UWB slot antenna, (b) UWB disc monopole antenna, c) Return loss characteristics. Antenna dimensions are in [mm].

by realistic scenarios in wearable sensor applications, we have chosen three distances between the body and the UWB antennas: 2, 5 and 10mm. It means that the human body lies well within the reactive near-field region (defined as in [30]) for considered antennas and frequencies between 3 and 8 GHz. For these three distances and all body models, we compare mass averaged (1 g) and unaveraged SAR values at 3, 6 and 8 GHz (within the frequency band where our UWB antennas operate). Since CST Microwave Studio compute mass-averaged SAR according to the algorithm in [31], we have implemented in Matlab our own algorithm to calculate 1 g SAR according to the IEEE standard C95.3-2002 [32]. Our main interest is to see the difference in SAR depending on the human body model, therefore all results were normalized to the SAR in the homogeneous muscle tissue model. Of course at different frequencies and distances those SAR values are not the same.

4.1. Peak SAR

In Fig. 2–4 we present calculated *ratio* ([dB]) of the peak SAR in layered models relative to the homogeneous muscle model for distances between UWB antennas and the body of 2, 5 and 10 mm, respectively. Each figure shows results for 3, 6 and 8 GHz. As mentioned above, all figures are normalized to the respective peak SAR in the muscle tissue model. These values are listed in Table 1.

Table 1. Peak SAR [W/kg] in the homogeneous muscle tissue model, $P_{in} = 1$ W.

UWB SLOT / **UWB MONOPOLE**			
	3 GHz	6 GHz	8 GHz
2 mm	*164* / 273	*139* / 143	*367* / 198
5 mm	*71* / 142	*48* / 62	*61* / 91
10 mm	*28* / 52	*18* / 16	*17* / 23

In all figures we see increased peak SAR in layered models, compared to the homogeneous body model. At the given frequency, the smallest SAR increase occurs at 2 mm distance between the antenna and body. For the UWB monopole antenna SAR increase at 3 GHz and 2 mm distance is smaller than 1.7 dB, but for the UWB slot antenna it is much higher (5.9 dB for the model with 1 mm thick skin and 9 mm thick fat tissue). Some explanations for this behavior will be given later on in the paper (Section 4.3). As the distance between antennas

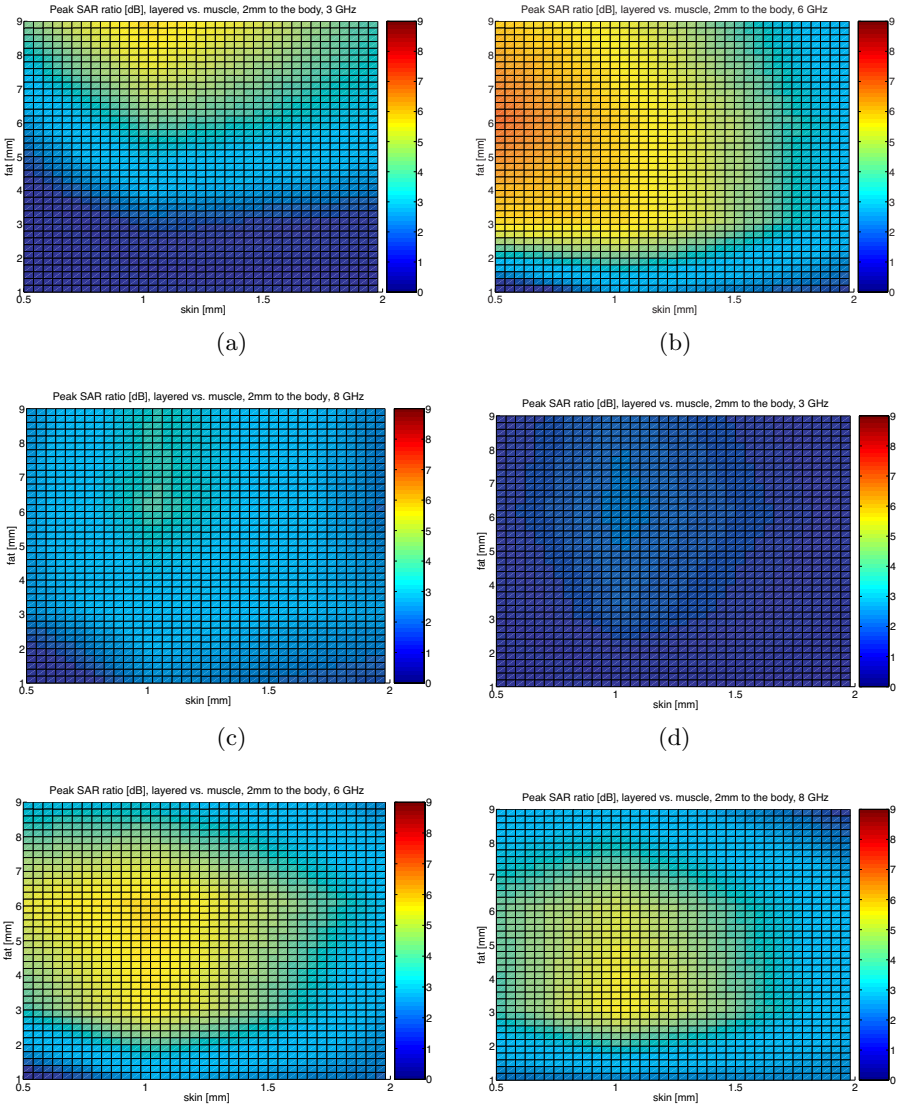

Figure 2. Ratio of peak SAR (no averaging mass) in the muscle and layered body models (0 dB equals SAR in muscle). Body 2 mm away. a) UWB slot @3 GHz (0 dB = 164 W/kg), b) UWB slot @6 GHz (0 dB = 139 W/kg), c) UWB slot @8 GHz (0 dB = 367 W/kg), d) UWB monopole @3 GHz (0 dB = 273 W/kg), e) UWB monopole @6 GHz (0 dB = 143 W/kg), f) UWB monopole @8 GHz (0 dB = 198 W/kg). $P_{in} = 1$ W.

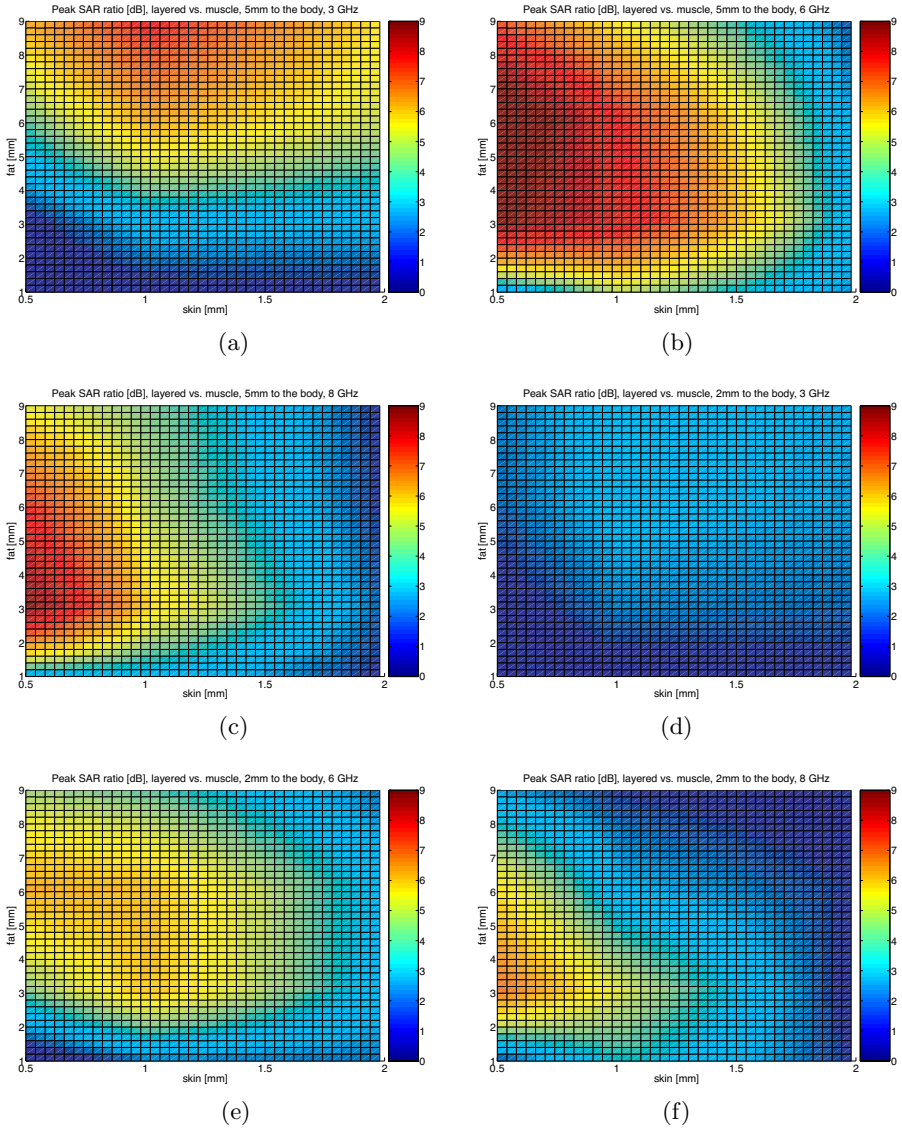

Figure 3. Ratio of peak SAR (no averaging mass) in the muscle and layered body models (0 dB equals SAR in muscle). Body 5 mm away. a) UWB slot @3 GHz (0 dB = 71 W/kg), b) UWB slot @6 GHz (0 dB = 48 W/kg), c) UWB slot @8 GHz (0 dB = 61 W/kg), d) UWB monopole @3 GHz (0 dB = 142 W/kg), e) UWB monopole @6 GHz (0 dB = 62 W/kg), f) UWB monopole @8 GHz (0 dB = 91 W/kg). $P_{in} = 1$ W.

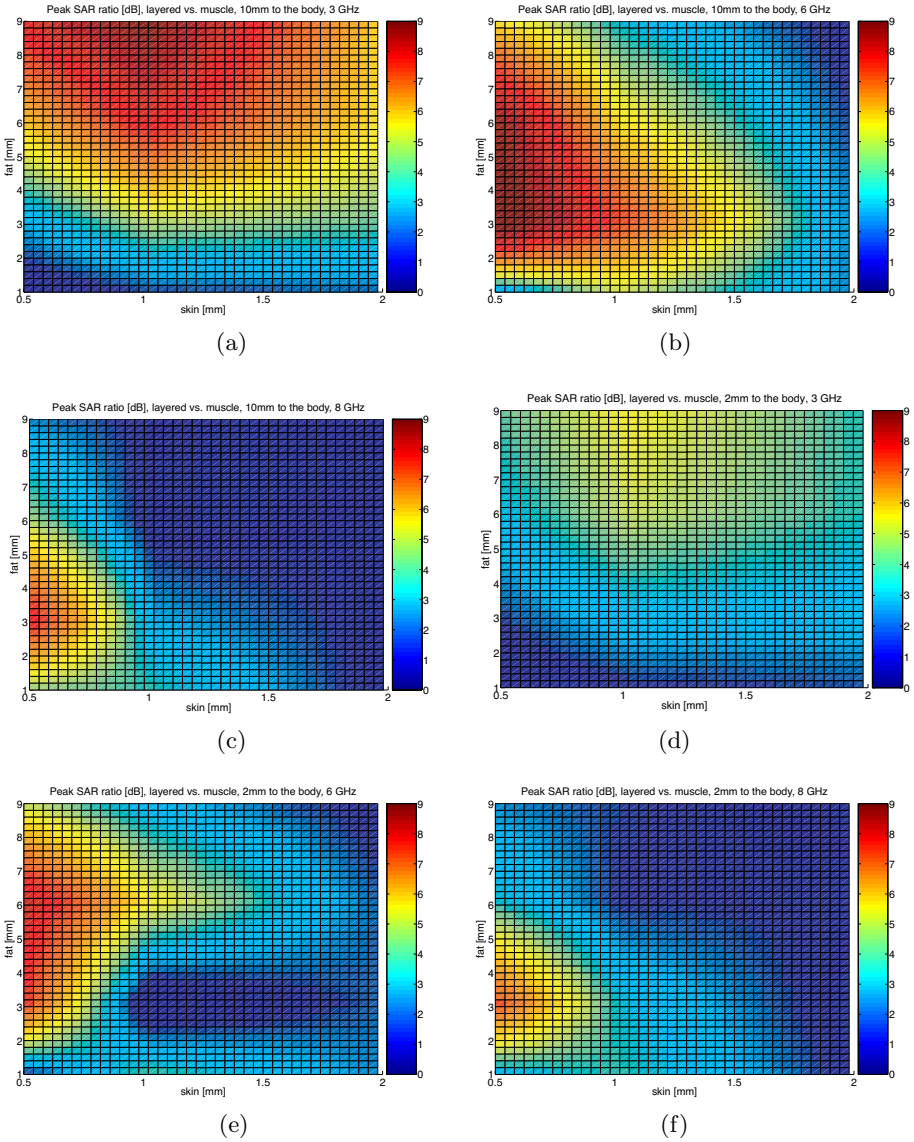

Figure 4. Ratio of peak SAR (no avera GHz (0 dB = 18 W/kg), c) UWB slot @8 GHz (0 dB = 17 W/kg), d) UWB monopole @3 GHz (0 dB = 52 W/kg), e) UWB monopole @6 GHz (0 dB = 16 W/kg), f) UWB monopole @8 GHz (0 dB = 23 W/kg). $P_{in} = 1$ W.

and body increases, also the SAR ratio grows at a certain frequency. Due to the high ϵ_r contrast between skin and fat layers (thus also high mismatch of their wave impedance), as well as high conductivity of the skin, in all investigated cases the maximum power absorption occurs in the skin layer. The absolute values of the unaveraged peak SAR can become as high as 930 W/kg (UWB slot, 2 mm distance, 8 GHz).

Comparing UWB slot and monopole antennas, we observe that as frequency and distance increases, maxima of the peak SAR ratios have similar value (see Fig. 4(c) and 4(f)). This behavior is actually not surprising (since for a very large distances we can consider radiated fields from both antennas being similar to the plane wave), but the small distance ($\sim\lambda/4$) where this phenomenon is already visible is rather surprising. Another similarity between two antennas, much more interesting, lies in the fact that actually if we look at peak SAR ratio figures, we clearly see regularity in their 'pattern'. Moreover, we observe that for both antennas maxima occur approximately for the same combination of the skin and fat tissue thicknesses (only at 3 GHz and 2 mm distance, Fig. 2(a) and 2(d), it is not the case). This phenomena will be analyzed in more details in the following paragraph.

4.2. Peak 1-g SAR

In Fig. 5–7 we present calculated *ratio* ([dB]) of the peak 1 g SAR in layered models relative to the homogeneous muscle model for distances between UWB antennas and the body of 2, 5 and 10 mm, respectively. Each figure shows results for 3, 6 and 8 GHz. In all figures values are normalized to the respective peak 1 g SAR in the muscle model. These values are listed in Table 2.

Table 2. Peak 1-g SAR [W/kg] in the homogeneous muscle tissue model, $P_{in} = 1$ W.

UWB SLOT **/ UWB MONOPOLE**			
	3 GHz	6 GHz	8 GHz
2 mm	*48.4* / 89.6	*37.1* / 62	*60.4* / 80.8
5 mm	*35.4* / 57.5	*21.7* / 27.7	*20.6* / 36.4
10 mm	*16.6* / 24.6	*8* / 7.8	*7.2* / 9.6

Since the peak 1 g SAR include spatial averaging of the absorbed energy, results in most cases are similar to those of unaveraged SAR. Namely, at the distance of 2 mm, there is maximally 1.4 dB 1 g SAR increase in layered model compared to the muscle model. But as we see

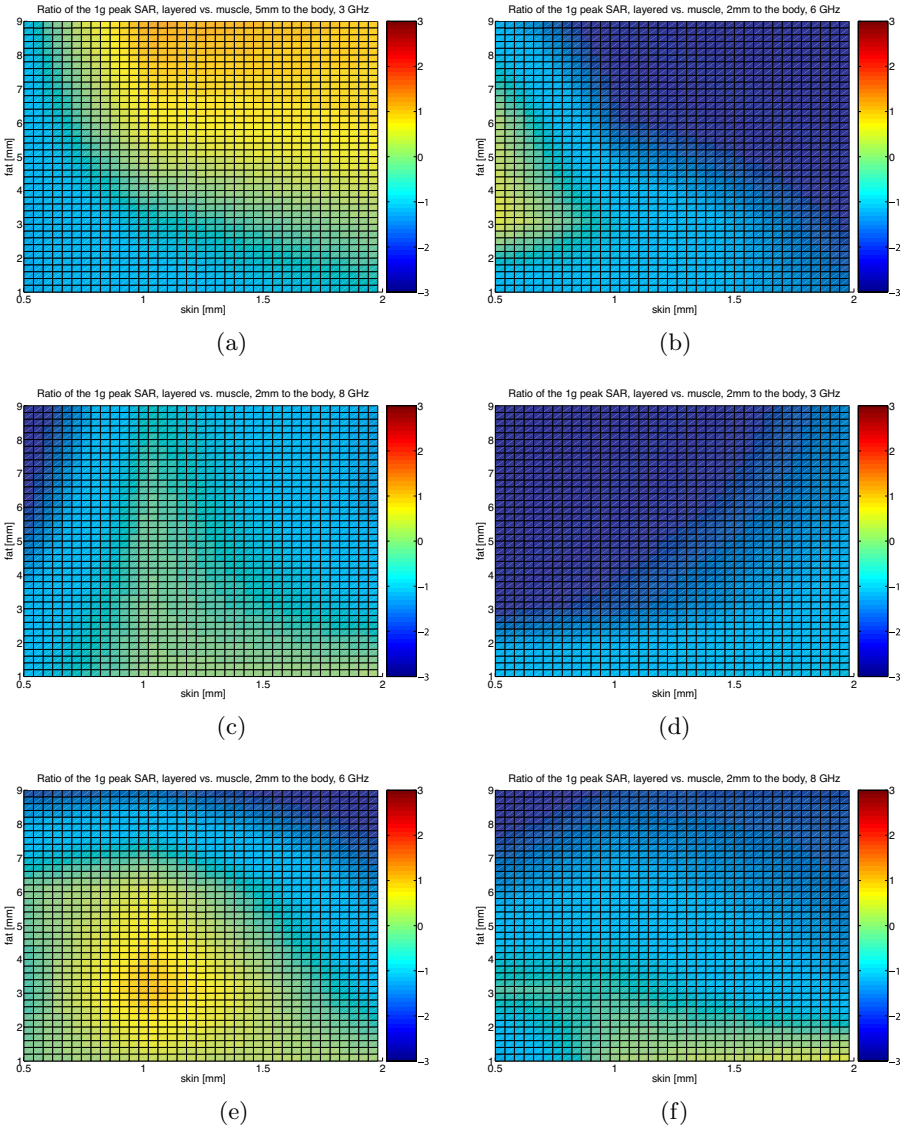

Figure 5. Ratio of 1 g peak SAR in the muscle and layered body models (0 dB equals SAR in muscle). Body 2 mm away. a) UWB slot @3 GHz (0 dB = 48.4 W/kg), b) UWB slot @6 GHz (0 dB = 37.1 W/kg), c) UWB slot @8 GHz (0 dB = 60.4 W/kg), d) UWB monopole @3 GHz (0 dB = 89.6 W/kg), e) UWB monopole @6 GHz (0 dB = 62 W/kg), f) UWB monopole @8 GHz (0 dB = 80.8 W/kg). $P_{in} = 1$ W.

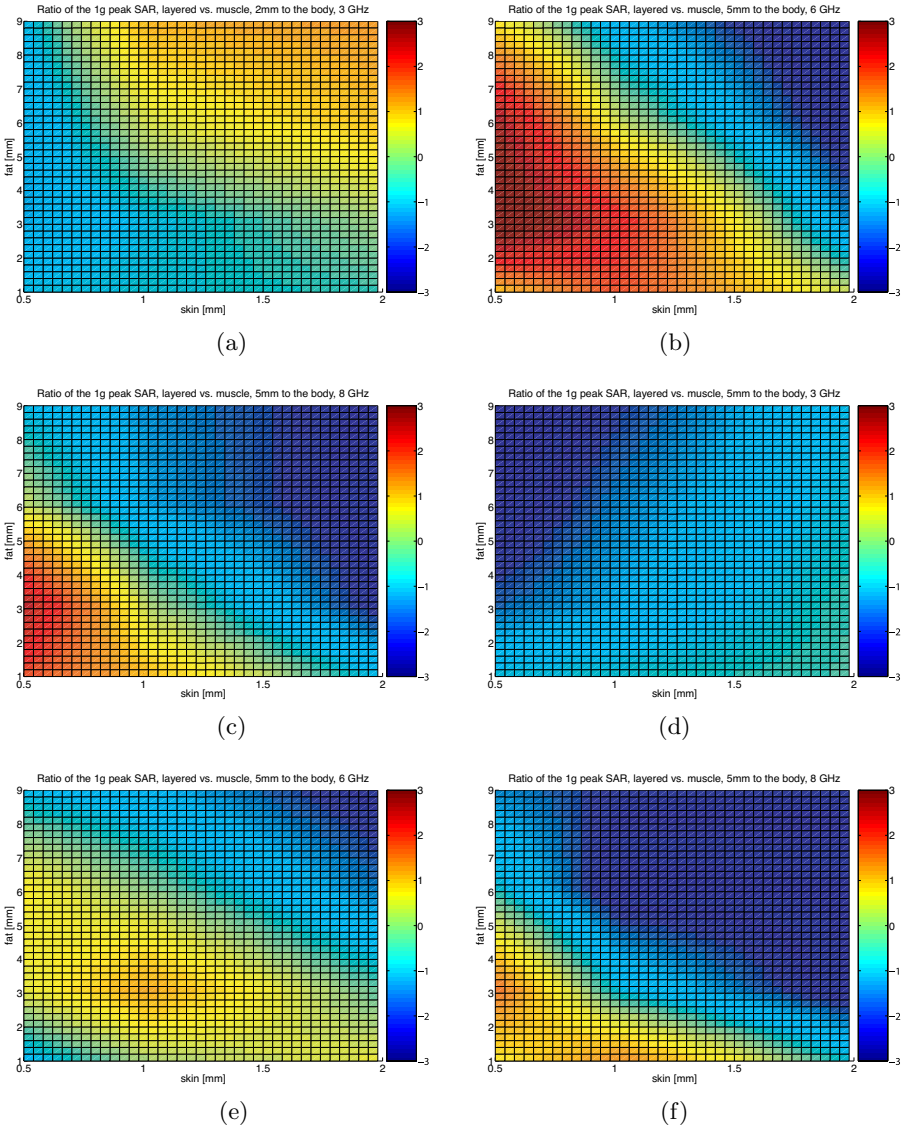

Figure 6. Ratio of 1 g peak SAR in the muscle and layered body models (0 dB equals SAR in muscle). Body 5 mm away. a) UWB slot @3 GHz (0 dB = 35.4 W/kg), b) UWB slot @6 GHz (0 dB = 21.7 W/kg), c) UWB slot @8 GHz (0 dB = 20.6 W/kg), d) UWB monopole @3 GHz (0 dB = 57.5 W/kg), e) UWB monopole @6 GHz (0 dB = 27.7 W/kg), f) UWB monopole @8 GHz (0 dB = 36.4 W/kg). $P_{in} = 1$ W.

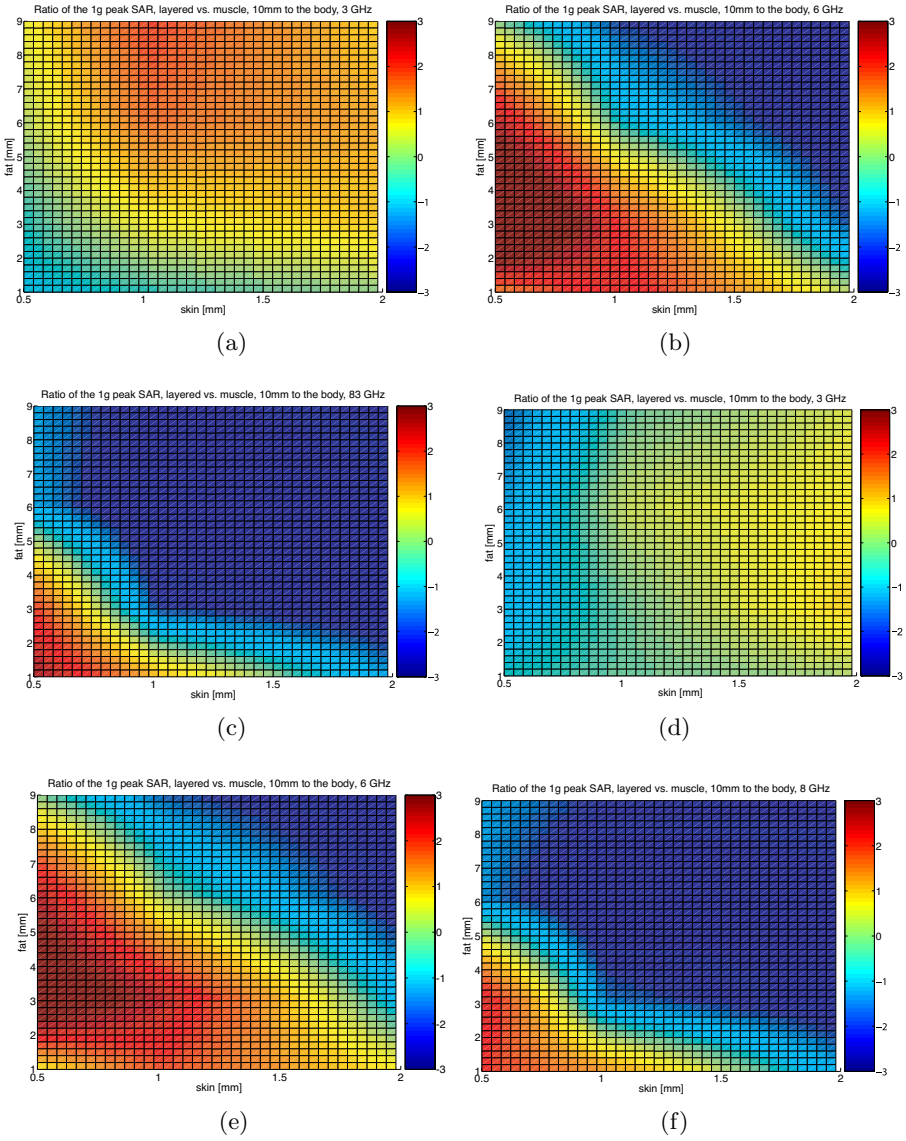

Figure 7. Ratio of 1 g peak SAR in the muscle and layered body models (0 dB equals SAR in muscle). Body 10 mm away. a) UWB slot @3 GHz (0 dB = 16.6 W/kg), b) UWB slot @6 GHz (0 dB = 8 W/kg), c) UWB slot @8 GHz (0 dB= 7.2 W/kg), d) UWB monopole @3 GHz (0 dB = 24.6 W/kg), e) UWB monopole @6 GHz (0 dB = 7.8 W/kg), f) UWB monopole @8 GHz (0 dB = 9.6 W/kg). $P_{in} = 1$ W.

in Fig. 6(b), already for a 5 mm distance peak 1 g SAR is 3 dB enhanced in the layered model. We also observe that at higher frequencies the 1 g SAR is increased only for a very thin skin tissue. It is so due to the high losses of the skin tissue and therefore less energy available for the layering resonance effect (described in more details in the Section 4.4).

It is interesting to compare 1 g SAR results for both investigated UWB antennas. We see that there is a bigger discrepancy between both antennas in a *pattern* of the averaged SAR, than for the unaveraged SAR. The maxima in figures with peak SAR for both antennas were observed for the similar skin and fat thickness in a layered model. But maxima of the 1 g SAR ratios occur in most cases for different layered model for the slot and monopole antenna. Only for 10 mm distance and frequency of 6 and 8 GHz results for both antennas are similar. Explanation of these differences will be given in a following paragraph.

4.3. Absorbed Power Density

In Tables 1 and 2 of preceding paragraphs we have seen that the absolute values of unaveraged and averaged SAR in the homogeneous muscle model can differ considerably between both antennas. To find out why is it so, we have examined the power density of absorbed energy just below (0.5 mm) the body surface. In Fig. 8 we present the absorbed power density at 3 GHz, for the homogeneous model as well as two layered models with the same skin thickness (1 mm) and fat thicknesses of 3 and 6 mm. Considering the muscle model, we see that there are two spots of the absorbed power for the slot antenna (Fig. 8(a)) and one for the monopole (Fig. 8(d)), in both cases due to the maxima of the antenna surface current [6]. It explains the 66% higher peak SAR for the monopole antenna, as well as 80% higher peak 1 g SAR (since peaks of the absorbed power are about 20 mm separated, and the 1 g mass averaging volume is about 10 mm). Interestingly, at 8 GHz we see (Tables 1, 2) that the unaveraged SAR is now 90% higher for the slot antenna, whereas the 1 g SAR is 33% higher for the monopole. After studying again power absorption (figures not shown), we observed that for the slot antenna peaks occur in the same places as at 3 GHz, but they are more intense due to increased frequency. For the monopole, at 8 GHz there are more resonances (e.g., in the ground plane and the disc), thus there is also more than one peak of the absorbed power. These peaks however are relatively close to each other, contributing to the spatially averaged SAR.

Results for layered models are shown in Fig. 8(b), 8(c) and Fig. 8(e), 8(f) for the slot and monopole antenna, respectively (normalized to the same value for each antenna). For the slot antenna,

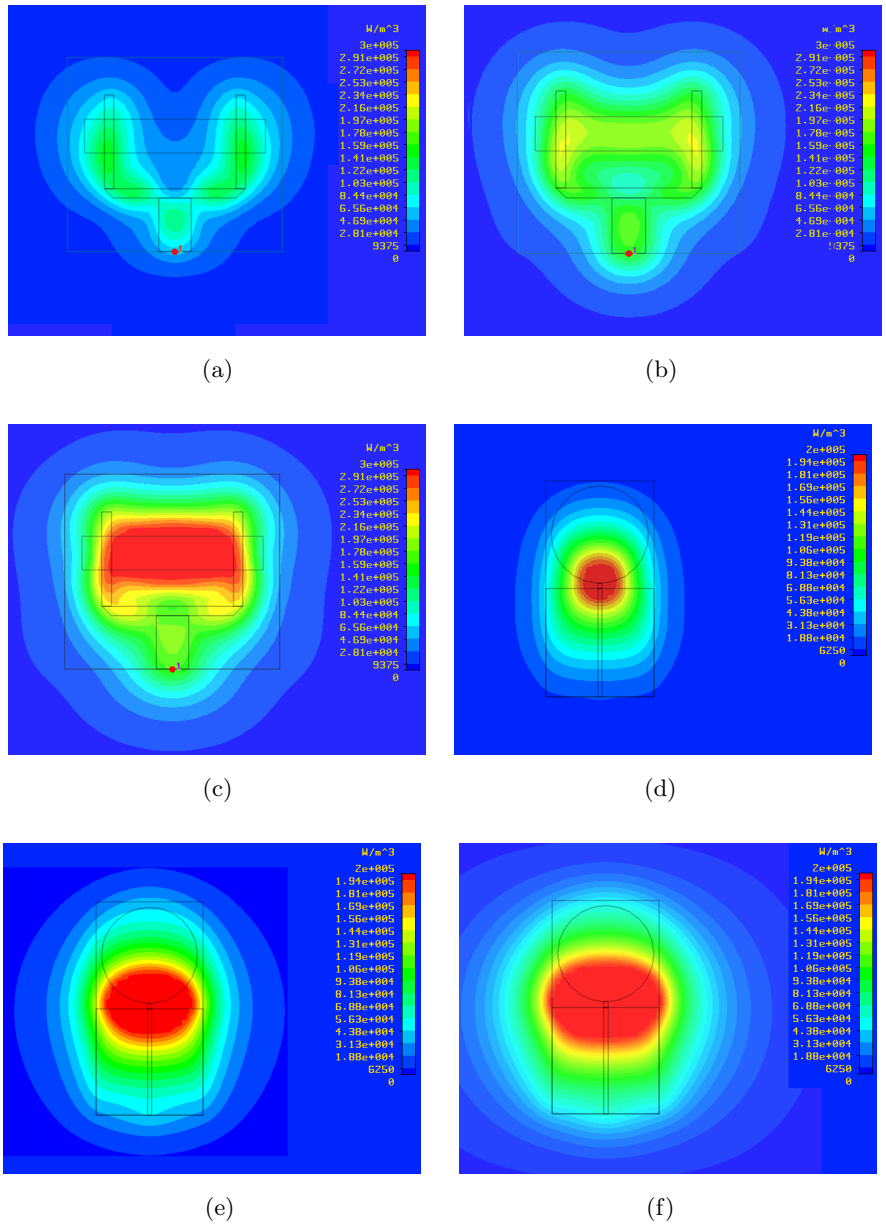

Figure 8. Absorbed power density (0.5 mm below the body surface) for the UWB slot antenna (upper figures) and UWB monopole antennas (lower figures) at 3 GHz, 2 mm away from the body: a) muscle tissue; b) fat 3 mm, skin 1 mm; c) fat 6 mm, skin 1 mm.

we see that two absorption peaks observed in the muscle model (Fig. 8(a)) are coming closer as the thickness of the fat tissue increases. For 6mm thick fat peaks have merged, resulting in about 6 dB higher unaveraged SAR, compared to the homogeneous muscle model. Also for the monopole antenna bigger losses in the skin occur for the thicker fat tissue. However the difference in the peak SAR between muscle and layered models is smaller (< 1.7 dB), because there is one absorption peak in all cases.

This effect of easier field penetration thru the skin tissue due to the thick fat tissue is caused by a lower effective dielectric constant of the layered model (e.g., at 3 GHz and normal incidence, for model with 1mm skin, 3mm fat $\epsilon_{r-eff} = 8.6 - i4.3$, for 1 mm skin, 6 mm fat $\epsilon_{r-eff} = 4.5 + i3.3$; calculations were done according to [3]). Easier coupling does not significantly increase 1 g SAR (but increase unaveraged SAR), because fat is a relatively low loss tissue and its bigger contribution in the averaging mass volume compensates higher peak SAR in the skin layer. Later on we will show that this absorption mechanism dominates only for very small ($< \lambda/25$) distances between the body and antenna.

5. STANDING WAVE EFFECT IN LAYERED TISSUES UNDER REACTIVE NEAR-FIELD EXPOSURE CONDITIONS

In this paragraph we report a standing wave effect of the electric field, which occur in layered biological tissues under reactive near-field exposure conditions. To our best knowledge, this effect was previously not reported in an open literature for such small separations between antennas and human body. Of course, for larger distances between an antenna and layered tissue this resonance effect is well known [3, 24]. But usually it was assumed that it does not occur in the reactive near-field region of the antenna, because the non-radiating (evanescent) fields dominate in this region.

As we wrote in the paragraph presenting peak SAR results (Section 4.1), for both antennas maxima occur approximately for the same layered model, at a given frequency. Therefore, we concluded that the peak SAR maxima must be related to the layered model structure and frequency. After a careful examination of electric fields in the layered body models at different frequencies and distances, we have indeed confirmed our suspicions. As an example in Fig. 9 we present the standing wave effect in the fat tissue, at 6 GHz and 5mm distance between layered model and the slot antenna. This case corresponds to the peak SAR results from Fig. 3(b). We see that for the 6mm

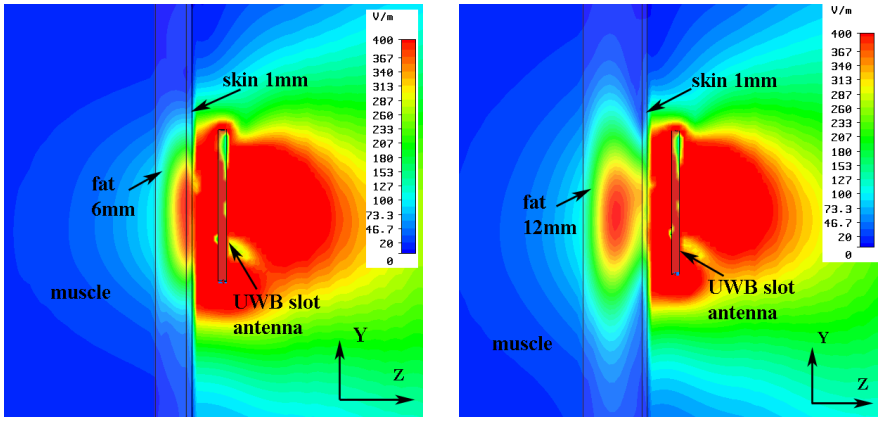

(a) (b)

Figure 9. Amplitude of the electric field ($|E|$) radiated by the UWB slot antenna in the vicinity of layered human body models: a) fat 6 mm, skin 1 mm; b) fat 12 mm, skin 1 mm. Frequency equals 6 GHz, distance between the antenna and body is 5 mm ($\lambda/10$).

thick fat layer, the maximum of $|E|$ occurs in the skin layer, close to the fat tissue (Fig. 9(a)). But when the fat thickness is doubled (12 mm), $|E|$ maximum exists in the fat tissue (Fig. 9(b)). This is a typical behavior when a standing wave occur. Maximum of power absorption lies still in the skin, since the fat losses are significantly lower than in a skin. After performing additional simulations for different scenarios (varying thicknesses of different layers, frequency as well as distance) we have found that this effect starts for distances between the antenna and body of about $\lambda/25$–$\lambda/20$. There is no sharp lower limit for the separation distance, because this effect does not only depend on the electrical distance between the antenna and body, but also on the content of reactive waves in the electric field spectrum of the antenna. The maximum of the absorbed power will be deposited in the skin layer when the fat thickness is around $\lambda/4$.

6. CONCLUSIONS

We presented studies concerning the electromagnetic energy absorption in different human body models due to body-worn UWB antennas, at frequencies of 3, 6 and 8 GHz. Typical small planar UWB antennas are used in this study: printed UWB disc monopole and

UWB slot antenna. Distances of 2, 5 and 10 mm (reactive near-field region) between antennas and human body were chosen, approximating realistic scenarios of operation in Wireless Body Area Networks. To approximate different parts of the human body, or body variations among different users, we compare results obtained for the planar homogeneous (muscle) model with those for three-layer body models (skin, fat and muscle tissues). For these body models we investigate the electromagnetic energy absorption mechanism by examining the peak 1 g SAR and peak SAR.

Results disclosed the increased peak SAR in all layered models, compared to the homogeneous body model. At the given frequency, the smallest SAR increase occurs at 2mm distance between the antenna and body. For the UWB monopole antenna peak SAR increases maximally 1.7 dB at 3 GHz and 2 mm distance, and for the UWB slot antenna it increases 5.9 dB. For larger distances peak SAR ratio can be as high as 9.5 dB, compared to the muscle model. The absolute values of the unaveraged peak SAR can become as high as 930 W/kg (UWB slot, 2 mm distance, 8 GHz). For the 1 g SAR results, at the distance of 2mm, there is maximally 1.4 dB increase in the layered model compared to the muscle model (in most cases it is lower). But already for a 5 mm distance, 1 g SAR is 3.3 dB enhanced in the layered model, and 4.3 dB for the 10mm separation.

Trying to explain above results, we have additionally studied basic absorption mechanism in human tissues, under the reactive near-field exposure conditions. We have found that for very small distances between the body and antenna ($< \lambda/25$), increased unaveraged SAR due to easier electric field penetration thru the skin tissue for body models with thick fat tissue, is caused by a lower effective dielectric constant of the layered model. But more serious effect of the layered composition of the human body is visible for distance between the antenna and body bigger than $\lambda/25$. In this case increased SAR is caused by the standing wave effect. This is rather surprising finding, because the body lies within the reactive near-field region of the antenna.

REFERENCES

1. Stuchly, M., "Electromagnetic fields and health," *IEEE Potentials*, Vol. 12, Issue 2, 34–39, Apr. 1993.
2. Rosen, A., M. A. Stuchly, and A. Vander Vorst, "Applications of RF/microwaves in medicine," *IEEE Transactions on Microwave Theory and Techniques*, Vol. 50, Issue 3, 963–974, March 2002.
3. Chatterjee, I., M. J. Hagmann, and O. P. Gandhi, "Electromag-

netic absorption in a multilayered slab model of tissue under near-field exposure conditions," *Bioelectromagnetics*, Vol. 1, Issue 4, 379–388, 1980.

4. Chatterjee, I., M. J. Hagmann, and O. P. Gandhi, "Plane-wave spectrum approach for the calculation of electromagnetic absorption under near-field exposure conditions," *Bioelectromagnetics*, Vol. 1, Issue 4, 363–377, 1980.
5. Kuster, N., "Multiple multipole method for simulating EM problems involving biological studies," *IEEE Transactions on Biomedical Engineering*, Vol. 40, Issue 7, 611–620, July 1993.
6. Kuster, N. and Q. Balzano, "Energy absorption mechanism by biological bodies in the near field of dipole antennas above 300 MHz," *IEEE Transactions on Vehicular Technology*, Vol. 41, Issue 1, 17–23, Feb. 1992.
7. Meier, K., V. Hombach, R. Kastle, R. Y.-S. Tay, and N. Kuster, "The dependence of electromagnetic energy absorption upon human-head modeling at 1800 MHz," *IEEE Transactions on Microwave Theory and Techniques*, Vol. 45, Issue 11, 2058–2062, Nov. 1997.
8. Lazzi, G., C. M. Furse, and G. P. Ghandi, "FDTD computation of electromagnetic absorption in the human head from mobile telephones," *Proc. of the 18th Annual Technical Meeting of the Bioelectromagnetics Society - BEMS*, 1996.
9. Christ, A. and N. Kuster, "Differences in RF energy absorption in the heads of adults and children," *Bioelectromagnetics*, September 2005.
10. Pitchers, S. M. and D.A. Eves, "A protocol for body centric networks," *IEE Eurowearable*, 87–92, Sept. 4–5, 2003.
11. Zasowski, T., F. Althaus, M. Stger, A. Wittneben, and G. Trster, "UWB for noninvasive wireless body area networks: Channel measurements and results," *IEEE Conference on Ultra Wideband Systems and Technologies, UWBST 2003*, Reston, Virginia, USA, Nov. 2003.
12. Hao, Y., A. Alomainy, P. S. Hall, Y. I. Nechayev, C. G. Parini, and C. C. Constantinou, "Antennas and propagation for body centric wireless communications," *2005. IEEE/ACES International Conference on Wireless Communications and Applied Computational Electromagnetics*, 586–589, April 3–7, 2005.
13. Chen, Z. N., X. H. Wu, H. F. Li, N. Yang, and M. Y. W. Chia, "Considerations for source pulses and antennas in UWB radio systems," *IEEE Transactions on Antennas and Propagation*,

Vol. 52, Issue 7, 1739–1748, July 2004.

14. Klemm, M., I. Z. Kovacs, G. F. Pedersen, and G. Troster, "Novel small-size directional antenna for UWB WBAN/WPAN applications," *IEEE Transactions on Antennas and Propagation*, December 2005.
15. Klemm, M. and G. Troster, "Integration of electrically small UWB antennas for body-worn sensor applications," *IEE Wideband and Multi-band Antennas and Arrays*, 141–146, 2005.
16. Chen, Z. N., A. Cai, T. See, and M. Chia, "Small planar UWB antennas in proximity of human head," *2005 IEEE International Conference on Ultra-Wideband (ICU 2005)*, Zurich, Switzerland, September 5–8, 2005.
17. Cai, A., T. See, and Z. N. Chen, "Study of human head effects on UWB antenna," *2005 IEEE International Workshop on Antenna Technology: Small Antennas and Novel Metamaterials (IWAT 2005)*, 310–313, March 7–9, 2005.
18. Alomainy, A., Y. Hao, C. G. Parini, and P. S. Hall, "Comparison between two different antennas for UWB on-body propagation measurements," *IEEE Antennas and Wireless Propagation Letters*, Vol. 4, 31–34, 2005.
19. Klemm, M., I. Locher, and G. Troster, "A novel circularly polarized textile antenna for wearable applications," *The 34rd European Microwave Conference (EuMC)*, Amsterdam, Netherlands, October 11–14, 2004.
20. Bharatula, N. B., M. Stger, P. Lukowicz, and G. Trster, "Empirical study of design choices in multisensor context recognition system," *IFAWC 2005: Proceedings of the 2nd International Forum on Applied Wearable Computing*, Zurich, Switzerland, March 17–18, 2005.
21. Kang, G. and O. P. Gandhi, "Effect of dielectric properties on the peak 1- and 10-g SAR for 802.11 a/b/g frequencies 2.45 and 5.15 to 5.85 GHz," *IEEE Transactions on Electromagnetic Compatibility*, Vol. 46, Issue 2, 268–274, May 2004.
22. Onishi, T. and S. Uebayashi, "Influence of phantom shell on SAR measurement in 3–6 GHz frequency range," *2004 International Symposium on Electromagnetic Compatibility*, 2004.
23. IT'IS Foundation, "Research projects — bio-electromagnetics and electromagnetic compatibility," available on-line: htt//www.iis.ee.ethz.ch/portrait/review/2004/BioEM04.pdf
24. Christ, A., A. Klingenboeck, and N. Kuster, "Energy absorption in layered biological tissue and its consequence on the compliance

testing of body-mounted wireless devices," *Progress in Electromagnetics Research Symposium 2005*, Hongzhou, China, August 23–26, 2005.

25. Kiveks, O., T. Lehtiniemi, and P. Vainikainen, "On the general energy-absorption mechanism in the human tissue," *Microwave and Optical Technology Letters*, Vol. 43, Issue 3, 195–201, Sept. 2004.
26. Klemm, M. and G. Troster, "Characterization of small planar antennas for UWB mobile terminals," *Wireless Communications and Mobile Computing*, Special Issue: Ultrawideband for Wireless Communications, Vol. 5, Issue 5, 501–597, August 2005.
27. Qing, X., M. Y. W. Chia, and X. Wu, "Wide-slot antenna for UWB applications," *IEEE Antennas and Propagation Symposium*, Vol. 1, 834–837, June 22–27, 2003.
28. Behdad, N., "A wideband multiresonant single-element slot antenna," *Antennas and Wireless Propagation Letters*, Vol. 3, 5–8, 2004.
29. htt//www.fcc.gov/fcc-bin/dielec.sh
30. Balanis, C. A., *Antenna Theory: Analysis and Design*, edition 2, Wiley, 1996.
31. Caputa, K., M. Okoniewski, and M. A. Stuchly, "An algorithm for computations of the power deposition in human tissue," *IEEE Antennas and Propagation Magazine*, Vol. 41, Issue 4, 102–107, Aug. 1999.
32. "IEEE Standard for Safety Levels With Respect to Human Exposure to Radiofrequency Electromagnetic Fields, 3 kHz to 300 GHz," IEEE Std. C95.1, 2002.